Computational Mechanics 27 (2001) 97–106 © Springer-Verlag 2001

A particle method for elastic and visco-plastic structures and fluid-structure interactions

Y. Chikazawa, S. Koshizuka, Y. Oka

Abstract A new particle method is proposed for elastic and visco-plastic structures based on the concept of MPS (Moving Particle Semi-implicit) method which was developed for fluid dynamics. Particle interaction models for differential operators are prepared in MPS method. The government equations of elastic structures are interpreted into interactions among particles. These interactions are equivalent to those of normal and tangential springs. Therefore the present particle method is simple and corresponding physical meaning is clear. Model for visco-plastic structure is represented to replace these elastic springs into visco-plastic ones. Elements or grids are not necessary. A tensile plate and a cantilever beam as elastic structures are analyzed by the present method. The results are in good agreement with theoretical solutions. Visco-plastic analysis for creep deformation and fracture of a cracked plate is also carried out and the result is in good agreement with an experiment. The present particle method for elastic structures is combined with MPS method for fluid-structural interaction problems. Since both methods are based on the same particle modeling in Lagrangian coordinates, large deformation of the interfaces can be easily analyzed. Water falling on a cantilever beam is analyzed by the combined method. Crash of water and resultant displacement of the beam are successfully analyzed. Structural analysis in a breakwater is carried out with wave propagation. The calculated pressure distribution on the breakwater is in good agreement with a theory.

1 Introduction

We need to analyze moving interfaces in fluid-structure interaction problems. The mesh will be distorted near the interfaces in the finite difference and the finite element methods and the calculation will stop when the displacement of the interfaces is large. Meshless methods are free from this difficulty. Besides, more and more complex geometries are required to analyze and mesh generation often takes more time than the structure analysis. Complex grid generation process will be much simplified in meshless methods. The meshless methods which have been developed for structural analysis are DEM (Diffused Element Method) (Nayroles et al., 1992), EFGM (Element Free Galerkin Method) (Belytchko et al., 1994) and FMM (Free Mesh Method) (Yagawa et al., 1996). DEM and EFGM employ moving least-square interpolants which need integral calculations on background cells. FMM is based on FEM (Finite Element Method) though it needs no explicit data of connectivity between nodes. FMM is developed for large scale analysis on parallel computers. Atluri et al. developed MLPG (Meshless Local Petrov-Galerkin) and LBIE (Local Boundary Integral Equation) methods (Atluri et al., 1998, 1999, 2000a, b, c; Zhu et al., 1998). These methods are truly meshless in the sense that they do not need a mesh either for interpolation purpose, or for the purpose of quadrature-integration of the energy.

MPS (Moving Particle Semi-implicit) method has been developed for incompressible flow analysis without elements. Moving interface problems, such as wave breaking, vapor explosions and boiling, were successfully analyzed using MPS method (Koshizuka and Oka, 1996, 1998 and 1999). MPS method has also been used for fluid-structural interaction. Chikazawa et al. (1999) calculated sloshing in an elastic tank which is treated as a thin structure represented by particles.

In the present study, a new particle method is proposed for thick elastic and visco-plastic structures based on the concept of MPS method which provides particle interaction models for differential operators. The governing equations of elastic structures are interpreted into interaction among particles. This method is combined with MPS method for fluid-structure interactions involving large deformation of interfaces.

2 Particle method for elastic structures

2.1 Governing equations

Governing equations for two-dimensional isotropic elastic structures are

$$\begin{aligned}(\lambda+\mu)\frac{\partial}{\partial x}\left(\frac{\partial u}{\partial x}+\frac{\partial v}{\partial y}\right)+\mu\left(\frac{\partial^2 u}{\partial x^2}+\frac{\partial^2 u}{\partial y^2}\right)&=-f_x\\(\lambda+\mu)\frac{\partial}{\partial y}\left(\frac{\partial u}{\partial x}+\frac{\partial v}{\partial y}\right)+\mu\left(\frac{\partial^2 v}{\partial x^2}+\frac{\partial^2 v}{\partial y^2}\right)&=-f_y\end{aligned} \quad (1)$$

where $\vec{u}=(u,v)$ is displacement vector and $\vec{f}=(f_x,f_y)$ is external force vector. λ and μ are constants that are expressed by

Received 21 November 2000

Y. Chikazawa (✉), S. Koshizuka, Y. Oka
Nuclear Engineering Research Laboratory,
The University of Tokyo, 22-2 Shirane, Shirakata,
Tokai-mura, Naka-gun, Ibaraki 319-1106, Japan

$$\lambda = \frac{vE}{(1+v)(1-v)} \tag{2}$$

$$\mu = \frac{E}{2(1+v)} \tag{3}$$

where E is Young's modulus and v is Poisson's ratio. The governing equations can be reduced to diffusion, rotation and volumetric strain terms.

$$\begin{aligned} 2\mu\nabla^2 u + \mu\frac{\partial}{\partial y}\left(\frac{\partial v}{\partial x} - \frac{\partial u}{\partial y}\right) + \lambda\frac{\partial}{\partial x}\left(\frac{\partial u}{\partial x} + \frac{\partial v}{\partial y}\right) &= -f_x \\ 2\mu\nabla^2 v - \mu\frac{\partial}{\partial x}\left(\frac{\partial v}{\partial x} - \frac{\partial u}{\partial y}\right) + \lambda\frac{\partial}{\partial y}\left(\frac{\partial u}{\partial x} + \frac{\partial v}{\partial y}\right) &= -f_y \end{aligned} \tag{4}$$

Each particle holds four variables: two components of the displacement vector $\vec{u} = (u, v)$, rotation $R = \nabla \times \vec{u}$ and divergence $D = \nabla \cdot \vec{u}$. Rewriting the equations in the matrix form, we have

$$\begin{pmatrix} 2\mu\nabla^2 & 0 & \mu\frac{\partial}{\partial y} & \lambda\frac{\partial}{\partial x} \\ 0 & 2\mu\nabla^2 & -\mu\frac{\partial}{\partial x} & \lambda\frac{\partial}{\partial y} \\ -\frac{\partial}{\partial y} & \frac{\partial}{\partial x} & -1 & 0 \\ \frac{\partial}{\partial x} & \frac{\partial}{\partial y} & 0 & 1 \end{pmatrix} \begin{pmatrix} u \\ v \\ R \\ D \end{pmatrix} = \begin{pmatrix} -f_x \\ -f_y \\ 0 \\ 0 \end{pmatrix} \tag{5}$$

2.2 Modeling to particle interaction

In the MPS method (Koshizuka and Oka, 1996), each particle interacts with its neighboring particles using a weighting function.

$$w(r) = \begin{cases} \frac{r_e}{r_{ij}} - 1 & r \le r_e \\ 0 & r > 0 \end{cases} \tag{6}$$

where r_{ij} is the distance between particles i and j, and r_e is the radius of weighting function (Fig. 1). The interaction area is limited by r_e. Particle number density at particle i is defined as

$$n_i = \sum_{j \neq i} w(r_{ij}) \tag{7}$$

The particle number density is constant at inside particles if the configuration of particles is uniform. This constant value is denoted by n^0. The particle number density decreases on boundaries because there are no particles outside.

Interactions between particles are averaged by the weighting function. Suppose f is an arbitrary variable, Laplacian at particle i is modeled as follows

$$\left(\nabla^2 f\right)_i = \sum_{j \neq i} 2d \frac{f_j - f_i}{r_{ij}^2} \frac{w(r_{ij})}{n_i} \tag{8}$$

where d is the number of space dimensions. Models for other differential operators, such as divergence, rotation and gradient, are as follows

$$\nabla \cdot \vec{f}_i = \sum_{j \neq i} \frac{(\vec{f}_j - \vec{f}_i) \cdot \vec{t}_{ij}}{r_{ij}} \frac{d}{n_i} w(r_{ij}) \tag{9}$$

$$\nabla \times \vec{f}_i = \sum_{j \neq i} \frac{(\vec{f}_j - \vec{f}_i) \cdot \vec{s}_{ij}}{r_{ij}} \frac{d}{n_i} w(r_{ij}) \tag{10}$$

$$\nabla f_i = \sum_{j \neq i} \frac{(f_j - f_i)}{r_{ij}} \vec{t}_{ij} \frac{d}{n_i} w(r_{ij}) \tag{11}$$

where $\vec{r}_{ij}$ is a position vector from particle i to j. $\vec{t}_{ij}$ is a unit vector parallel to $\vec{r}_{ij}$ and $\vec{s}_{ij}$ is a unit vector perpendicular to $\vec{r}_{ij}$ (Fig. 2). More details of the particle interaction models are explained in a reference (Koshizuka and Oka, 1996). The rotation model (Eq. (10)) is newly developed in the present study.

In SPH (Smoothed Particle Hydrodynamics) (Gingold and Monaghan, 1982), which was developed for compressible flow analysis, another gradient model has been used.

$$\nabla f_i = \sum_{j \neq i} \frac{(f_j + f_i)}{2r_{ij}} \vec{t}_{ij} \frac{d}{n_i} w(r_{ij}) \tag{12}$$

Corresponding to this gradient model, another rotation model is also developed in the present study as

$$\nabla \times \vec{f}_i = \sum_{j \neq i} \frac{(\vec{f}_j + \vec{f}_i) \cdot \vec{s}_{ij}}{2r_{ij}} \frac{d}{n_i} w(r_{ij}) \tag{13}$$

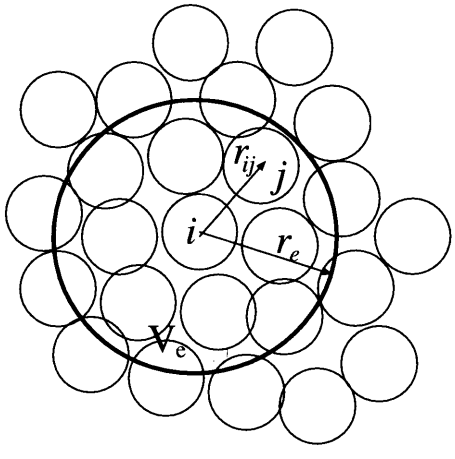

Fig. 1. Neighboring particles

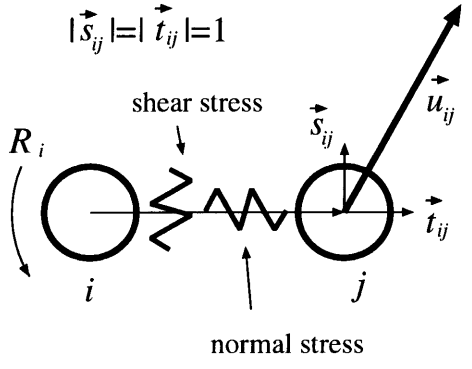

Fig. 2. Particle model

Using the above Laplacian model (Eq. (8)), the diffusion terms in the government equations of elastic structures are discretized to,

$$\left(\nabla^2 u\right)_i = \sum_{j\neq i} \frac{2d}{n^0}\left(\frac{u_j - u_i}{r_{ij}^2}\right) w(r_{ij})$$
$$\left(\nabla^2 v\right)_i = \sum_{j\neq i} \frac{2d}{n^0}\left(\frac{v_j - v_i}{r_{ij}^2}\right) w(r_{ij}) \tag{14}$$

The interactions are normalized by n^0 in place of n_i to consider boundary conditions. Boundary conditions will be explained in the next subsection. Using Eqs. (9) and (10), divergence and rotation at particle i are expressed respectively as

$$D_i = \sum_{j\neq i} \frac{(\vec{u}_j - \vec{u}_i)\cdot \vec{t}_{ij}}{r_{ij}} \frac{d}{n_i} w(r_{ij}) \tag{15}$$

$$R_i = \sum_{j\neq i} \frac{(\vec{u}_j - \vec{u}_i)\cdot \vec{s}_{ij}}{r_{ij}} \frac{d}{n_i} w(r_{ij}) \tag{16}$$

The governing equations are transformed to

$$\sum_{j\neq i}\left[2\mu\left\{\frac{u_j - u_i}{r_{ij}^2}\right\} + \left\{-\mu\frac{(R_i + R_j)/2}{r_{ij}} s_{ij,x} + \lambda\frac{(D_i + D_j)/2}{r_{ij}} t_{ij,x}\right\}\right]\frac{2d}{n^0} w(r_{ij}) = -f_x$$
$$\sum_{j\neq i}\left[2\mu\left\{\frac{v_j - v_i}{r_{ij}^2}\right\} + \left\{-\mu\frac{(R_i + R_j)/2}{r_{ij}} s_{ij,y} + \lambda\frac{(D_i + D_j)/2}{r_{ij}} t_{ij,y}\right\}\right]\frac{2d}{n^0} w(r_{ij}) = -f_y \tag{17}$$

The third terms of the left side represent the volumetric stress components which are determined by gradient of D_i. The gradient model of Eq. (12) is applied to these terms. The second terms of left side represent removal of rotation from the shear stress components. The rotation model of Eq. (13) is applied to these terms.

The matrix of the left side of Eq. (5) is completely discretized to Eq. (17) by the particle interaction models. The matrix equation can be solved by a solver, for example, SOR method. This means that the present method can be applied to static problems (Chikazawa et al., 1999). Dynamic problems can be solved explicitly by using the transient governing equation (Koshizuka et al., 1999).

Displacement of particle j from particle i is $\vec{u}_j - \vec{u}_i$. The displacement vector can be reduced to a perpendicular component $(\vec{u}_j - \vec{u}_i)\cdot\vec{s}_{ij}\vec{s}_{ij}$ and a parallel component $(\vec{u}_j - \vec{u}_i)\cdot\vec{t}_{ij}\vec{t}_{ij}$. Equation (14) can be rewritten to

$$\left(\nabla^2 u\right)_i = \frac{2d}{n^0}\sum_{j\neq i}\left\{\frac{(\vec{u}_j - \vec{u}_i)\cdot\vec{t}_{ij}}{r_{ij}^2} t_{ij,x} + \frac{(\vec{u}_j - \vec{u}_i)\cdot\vec{s}_{ij}}{r_{ij}^2} s_{ij,x}\right\} w(r_{ij})$$
$$\left(\nabla^2 v\right)_i = \frac{2d}{n^0}\sum_{j\neq i}\left\{\frac{(\vec{u}_j - \vec{u}_i)\cdot\vec{t}_{ij}}{r_{ij}^2} t_{ij,y} + \frac{(\vec{u}_j - \vec{u}_i)\cdot\vec{s}_{ij}}{r_{ij}^2} s_{ij,y}\right\} w(r_{ij}) \tag{18}$$

According to Eq. (18), two particles behave as if they are connected by two springs: normal and shear springs which are governed by the parallel and perpendicular components of displacement, respectively (Fig. 2). A normal stress σ_{ij} and a shear stress τ_{ij} are given with respect to the position vector from particle i to j. These two stresses are obtained from stress tensor $\bar{\sigma}$ as follows

$$\bar{\sigma}\cdot\vec{t}_{ij} = \begin{bmatrix}\sigma_x & \tau_{xy}\\ \tau_{xy} & \sigma_y\end{bmatrix}\vec{t}_{ij} = \sigma_{ij}\vec{t}_{ij} + \tau_{ij}\vec{s}_{ij} \tag{19}$$

The normal stress can be written as

$$\sigma_{ij} = 2\mu\frac{(\vec{u}_j - \vec{u}_i)\cdot\vec{t}_{ij}}{r_{ij}} + \lambda\frac{D_i + D_j}{2} \tag{20}$$

The first term of the right side represents a normal spring and the second term represents pressure. The shear stress between two particles is calculated by

$$\tau_{ij} = 2\mu\frac{(\vec{u}_j - \vec{u}_i)\cdot\vec{s}_{ij}}{r_{ij}} - \mu\frac{R_i + R_j}{2} \tag{21}$$

Rotating motion is removed from the perpendicular displacement.

2.3 Boundary conditions

(a) Free boundary

Stress components are zero on free boundaries.

$$\bar{\sigma}\cdot\vec{n} = \vec{0} \tag{22}$$

where $\vec{n}$ is the unit normal vector to the free boundary surface.

We assume that a particle i exists at the boundary and a temporal particle j is located outside where $\vec{n} = (\vec{r}_j - \vec{r}_i)/(|\vec{r}_j - \vec{r}_i|)$ is normal to the free boundary. When particle interactions are normalized by n^0 as Eqs. (14) and (17), there is no interaction with the outside particles. On the other hand, when the interactions are normalized by n_i as Eqs. (15) and (16), the interaction with the outside particle is the same as that with the inside particle. This boundary condition is simple but may cause some error since the interaction is averaged within the weighting function. Finally Eq. (22) is reduced to

$$\vec{u}_j - \vec{u}_i = 0$$
$$D_j = 0 \tag{23}$$
$$R_j = 0$$

with respect to the temporal particles

(b) fixed boundary

At fixed boundaries, Dirichlet boundary conditions are given. Temporal particles are also considered as the same

way as the free boundary. Displacement, divergence and rotation of temporal particle j are given as follows

$$\vec{u}_j = 0$$
$$D_j = 0 \tag{24}$$
$$R_j = 0$$

3 Particle method for elasto-visco-plastic structures

The model for visco-plastic structures focused on here is

$$\dot{\epsilon}_{\mathrm{vp}} = \gamma\left(\sigma - \sigma_Y - H\epsilon_{\mathrm{vp}}\right) \tag{25}$$

where γ is the reciprocal of the viscosity coefficient, H is the stiffness coefficient and σ_Y is the yield stress. Strain between particles i and j is discretized as follows

$$\epsilon_{\mathrm{vp},ij} = \frac{u_{\mathrm{vp},j} - u_{\mathrm{vp},i}}{r_{ij}} \tag{26}$$

where u_{vp} is visco-plastic replacement. Equation (25) is discretized as follows

$$\frac{\epsilon_{\mathrm{vp},ij} - \epsilon^{\mathrm{old}}_{\mathrm{vp},ij}}{\mathrm{d}t} = \gamma\left(\sigma - \sigma_Y - H\frac{\epsilon_{\mathrm{vp},ij} + \epsilon^{\mathrm{old}}_{\mathrm{vp},ij}}{2}\right) \tag{27}$$

where $\epsilon^{\mathrm{old}}_{\mathrm{vp},ij}$ is the strain at the old timestep. When particles are moved by Lagrangian description, $\epsilon^{\mathrm{old}} = 0$. H is assumed to be zero in this study. Equation (27) is reduced to

$$\epsilon_{\mathrm{vp},ij} = \mathrm{d}t\,\gamma(\sigma - \sigma_Y) \tag{28}$$

This equation is similar to elasticity $\epsilon = E^{-1}\sigma$ substituting E by $E_{\mathrm{vp}} = \frac{1}{\Delta t\gamma}$.

First, elastic calculation is performed. The particles that satisfy Von Mises' yield condition are regarded as visco-plastic. Next, plastic calculation is performed. Total strain is expressed by

$$\mathrm{d}\vec{\epsilon} = \mathrm{d}\vec{\epsilon}_{\mathrm{e}} + \mathrm{d}\vec{\epsilon}_{\mathrm{vp}} \tag{29}$$

where $\vec{\epsilon}_e$ and $\vec{\epsilon}_{\mathrm{vp}}$ are elastic and visco-plastic strain, respectively.

4 Test calculations for elastic Structures

4.1 Tensile plate

First, a tensile plate is analyzed. The calculation geometry is shown in Fig. 3. The Young's modulus E is 10^7 (kg cm^{-1} s^{-2}) and Poisson's ratio is 0.3. The number of particles is 289 and $r_e = 3.0l_0$ where l_0 is the distance between adjacent particles. A particle at the center of the plate is fixed. Top and bottom sides of the plate are free boundaries. Normal stress is loaded symmetrically on both left and right sides using this equation

$$\sigma = \sigma_0\left\{1 - \left(\frac{y}{16}\right)^2\right\} \tag{30}$$

where σ_0 is 1000 (kg cm^{-1} s^{-2}). The calculated and analytical displacement distributions on $x = 32$ are shown in Fig. 4. The numerical result is in good agreement with analytical one.

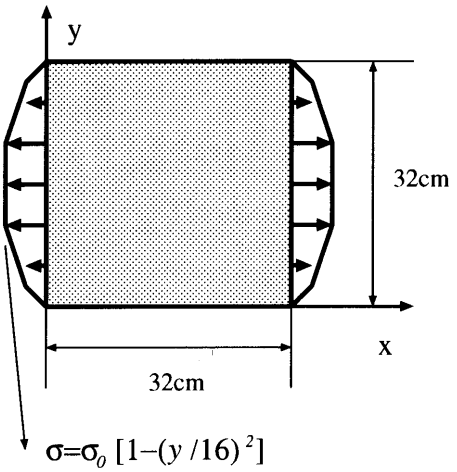

Fig. 3. Geometry for a tensile plate

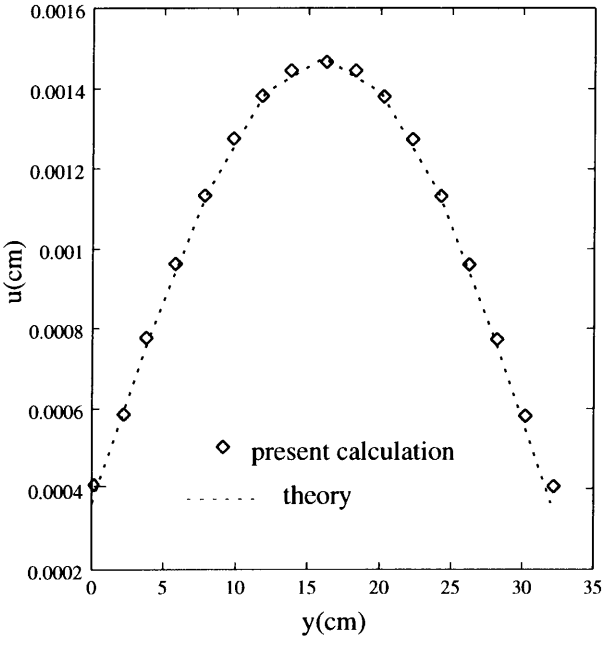

Fig. 4. Replacement of the tensile plate

4.2 Cantilever beam

Next, a cantilever beam is calculated. The geometry is shown in Fig. 5. The beam is supported at $x = 0$ and external force is loaded uniformly at $x = 4.0$. To compare with an analytical solution, a fixed boundary conditions is given as

$$u(y) = -6\frac{P}{Eh^3}\frac{2+v}{3}y^3$$
$$v(y) = -2\frac{P}{Eh^3}\left\{3vly^2\right\} \tag{31}$$

The number of particles is changed from 85 to 4257 with $r_e = 3.0l_0$.

The calculated displacement at $y = 0.5$ is shown in Fig. 6 where the number of the particles is 153. The

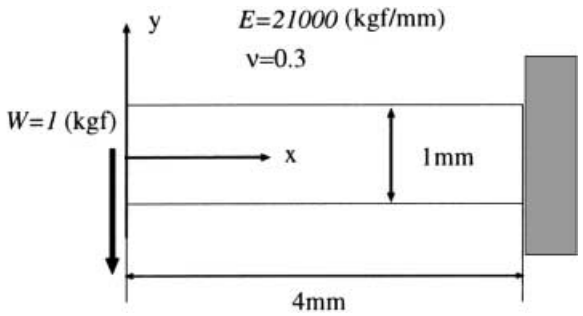

Fig. 5. Geometry for a cantilever beam

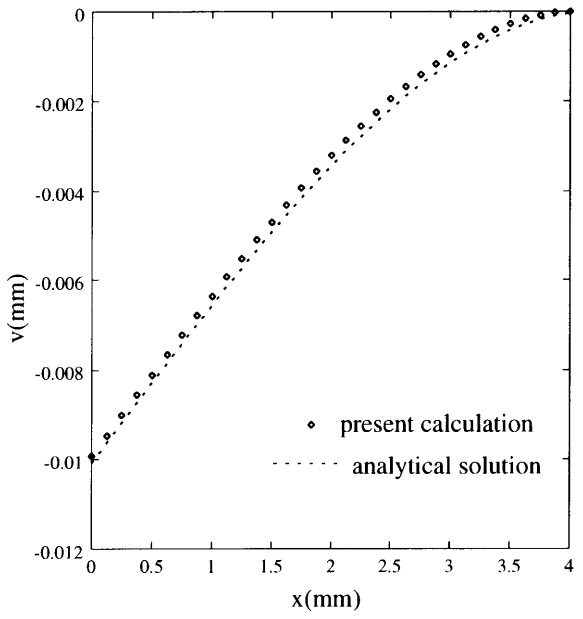

Fig. 6. Replacement of a cantilever beam

numerical result is in good agreement with the analytical solution. Errors are plotted against the number of particles in Fig. 7 in comparison with those of EFGM (Element Free Galerkin Method) (Nagashima et al., 1996) and FEM (Yang, 1986). EFGM is one of meshless methods. This FEM uses rectangular elements of 4 nodes and each node has 2 degrees of freedom. The error of the present method is smaller than that of EFGM and larger than that of FEM. The error decreases below 1% when using 200 particles. Normal and shearing stress distributions at $y = 0$ are shown in Fig. 8 and those of below at $x = 2.0$ in Fig. 9. These results agree with analytical solutions but there are differences near the boundaries. This suggests that the present method of boundary conditions leads to errors.

5
Result of elasto-visco-plastic calculation

5.1
Analysis of a visco-plastic tensile bar

The geometry is shown in Fig. 10. The length and width of the bar are 10.0 and 2.5 mm, respectively. The bar is fixed at the top and loaded uniformly 30 N/mm^2 at the bottom. Young's modulus is 10000 N/mm^2 and Poisson ratio is 0.0. H and γ is 0.0 and 0.001 day^{-1}, respectively. The bar is

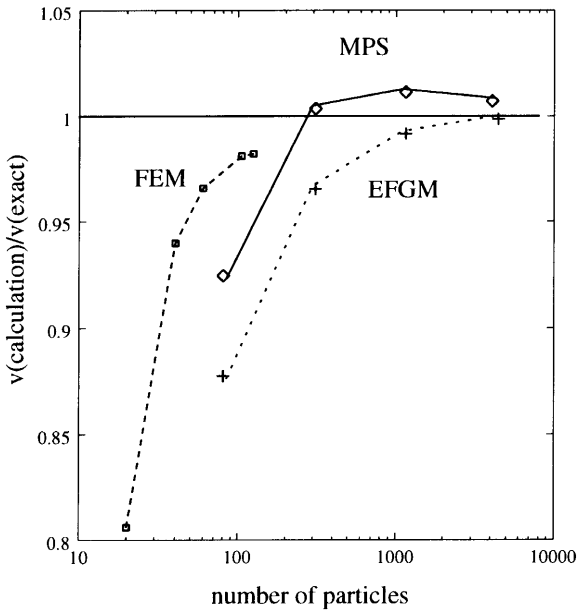

Fig. 7. Errors in cantilever beam calculations

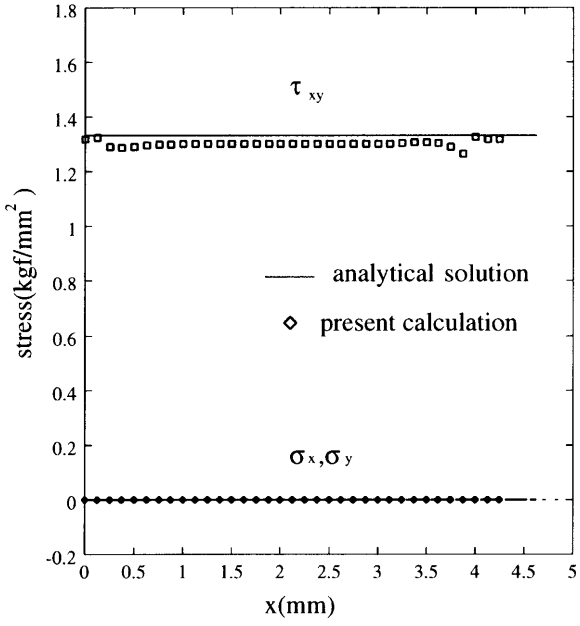

Fig. 8. Distributions of stress components at $y = 0$

completely yield and visco-plastic replacement is increased against time. Figure 11 is the calculated replacement at the bottom. The result is in good agreement with analytical one.

5.2
Analysis of a creep crack

An analysis for a creep crack is carried out. The geometry of the calculation is shown in Fig. 12. The width, length and thickness of the plate are 320, 480 and 1 mm, respectively. The crack length is 128 mm. Young's modulus is 206 GPa and Poisson ratio is 0.3. Yield stress is 431 MPa and γ is 0.01 h^{-1}. The plate is loaded symmetrically from the top and bottom.

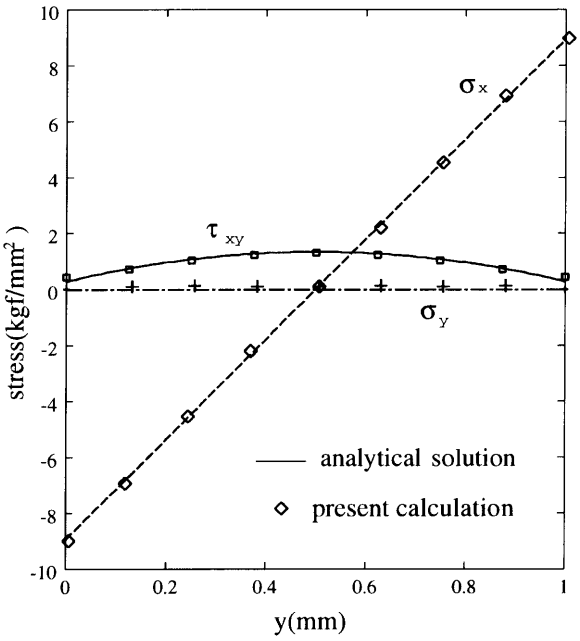

Fig. 9. Distributions of stress components at $x = 2.0$

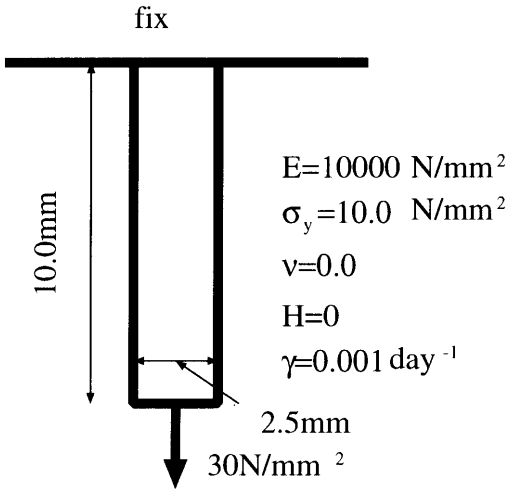

Fig. 10. Geometry for a visco-plastic bar

The deformation of the plate is shown in Fig. 13. A white particle means elastic and black one does visco-plastic. The line at the center of the plate shows initial crack. Particle interactions across the crack is set to zero. The deformation of the plate becomes larger and larger under the constant load and breaks eventually.

Experimental analysis of creep cracks was studied by Yokobori et al. [16]. They used smooth, notched (DEN) and precracked (CT) specimens. They showed the existence of a master curve for creep deformation. The normalized replacement Φ for smooth specimens is

$$\Phi = 0.4(\epsilon - \epsilon_0) \ , \tag{32}$$

for DEN specimens

$$\Phi = \frac{4\Delta\phi}{\phi_0} \ , \tag{33}$$

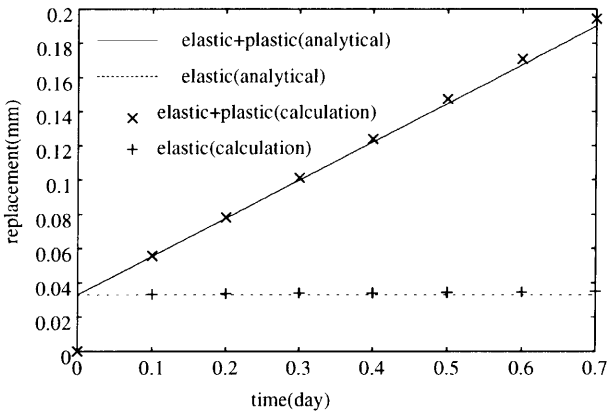

Fig. 11. Replacement of a visco-plastic bar

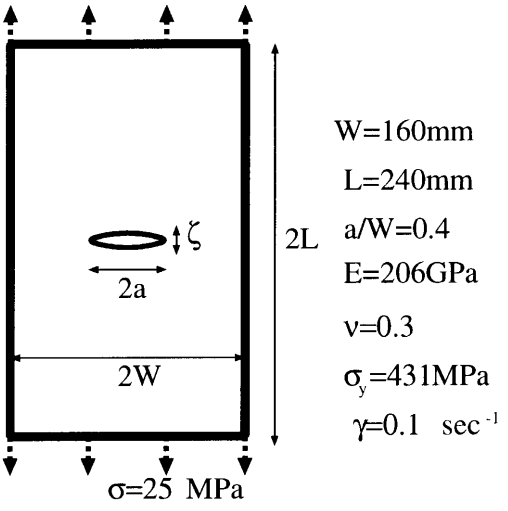

Fig. 12. Geometry of a cracked plate

for CT specimens

$$\Phi = \frac{\Delta\delta}{\delta_0} \tag{34}$$

where ϕ and δ are notch opening and load-line displacement respectively. The calculated replacement is normalized as follows

$$\Phi = 0.25\frac{\zeta - \zeta_0}{\zeta_0} \tag{35}$$

where ζ is defined in Fig. 14. Normalized replacement versus time normalized by fracture time t_f is compared with experiment in Fig. 15. Although there is a little difference around $t/t_f = 0.9$, the calculated result is in good agreement with that of experimental.

6
Analysis of fluid-structural interaction

6.1
Water falling on cantilever beam

The present method for structures is applicable to fluid-structural interaction problems involving large deformation of interfaces. Fluid and structures are analyzed by

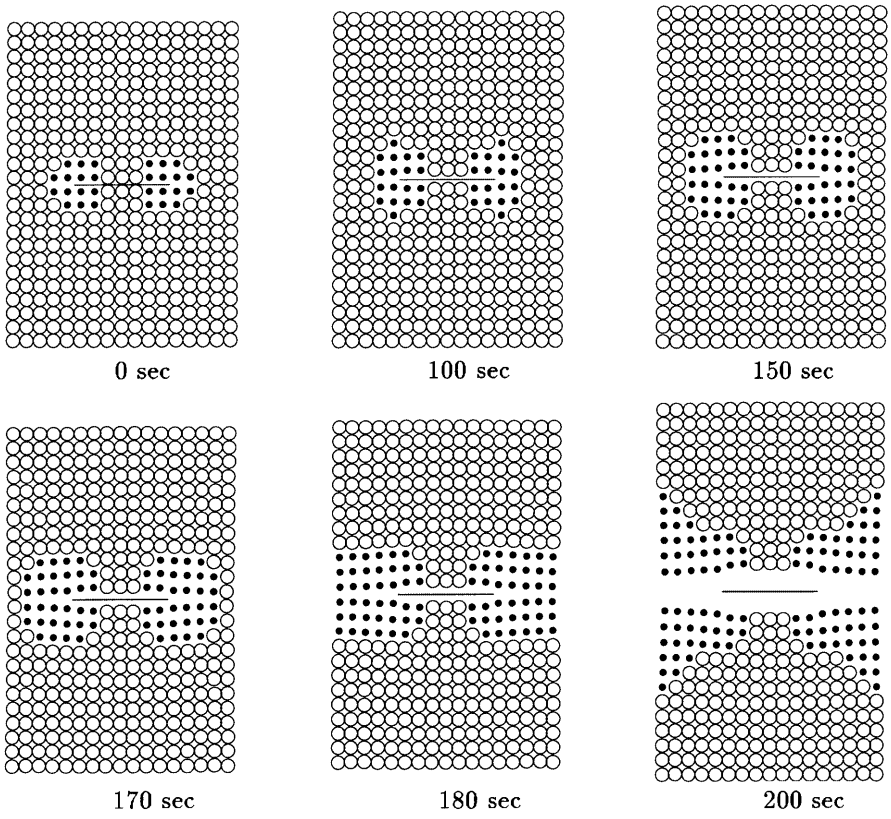

Fig. 13. Deformation of a cracked plate

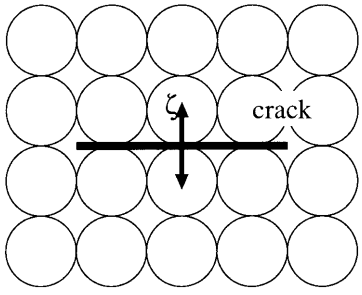

Fig. 14. Definition of zeta

MPS and the present method, respectively. Pressure distributions on the structures are obtained by the fluid flow analysis and they are used as the boundary condition in the structure analysis. In the structural calculation, elastic particles are directly moved according to the displacement as fully Lagrangian description. The moved elastic particles are treated as a fixed wall in the fluid calculation. However in this calculation displacement of the structure is small enough to neglect. Only the free surface of the fluid suffer large deformation.

Figure 16 shows the geometry of the present problem of fluid-structural interaction. A water drop impinges on to a cantilever beam and displacement in the beam is solved. The number of particles is 474 and the time step is 1.0×10^{-3}. Figure 17 shows the calculated displacement in the beam. The water drop is largely deformed, which can be calculated by MPS method. In FEM, modeling of the contact between the fluid and the beam is generally complex. In the particle methods, the particles begin interaction when they are closer than r_e.

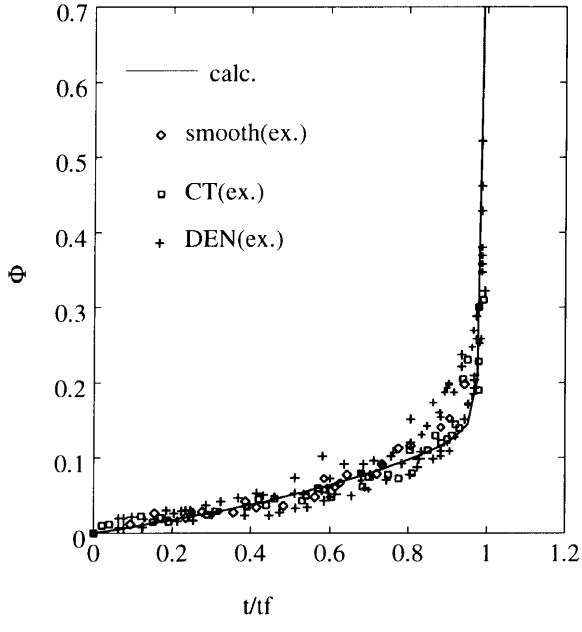

Fig. 15. Deformation vs. time

6.2
Waves propagation against a breakwater

The geometry is shown in Fig. 18. Waves are generated by a vertical wall, called wave maker, which moves as follows

$$A(x) = A_0 \sin(t/T) \tag{36}$$

where A_0 is 0.01 (m) and T is 1.0 (s). The number of particles is 5878 and the time step is 2.0×10^{-3} using Runge– Kutta scheme. Using this scheme, we can make the

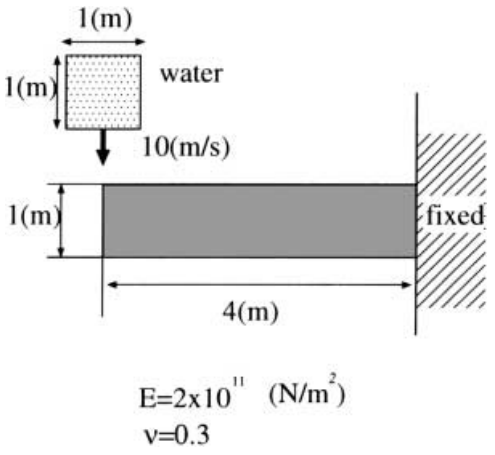

Fig. 16. Collision of water and a beam

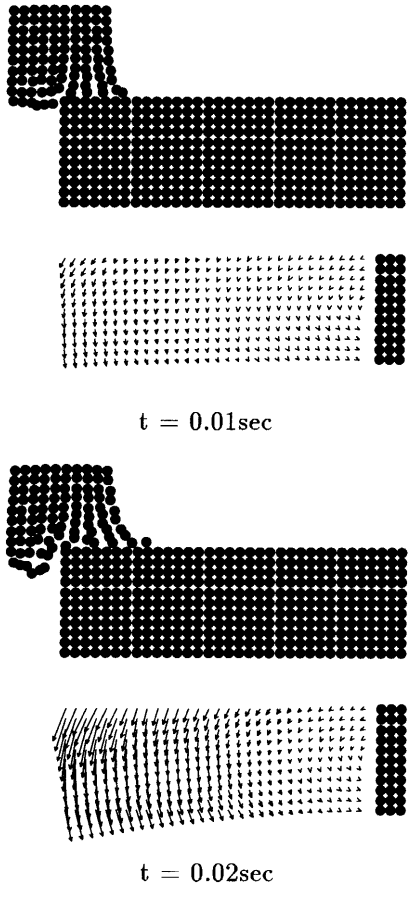

Fig. 17. Distribution of particles and displacement ($\times 10^8$) of a beam

pressure calculation more stable. The waves propagate as shown in Fig. 19. The shape of the waves is that of clapotis which does not causes wave breaking. MPS method can solve wave breaking as well as larger deformation of the waves (Koshizuka 1998). In this calculation, wave breaking is not solved since and the calculated wave breaking can not be compared with analytical solution.

The calculated wave height at the breakwater is shown in Fig. 20. Total force loaded on the breakwater is shown

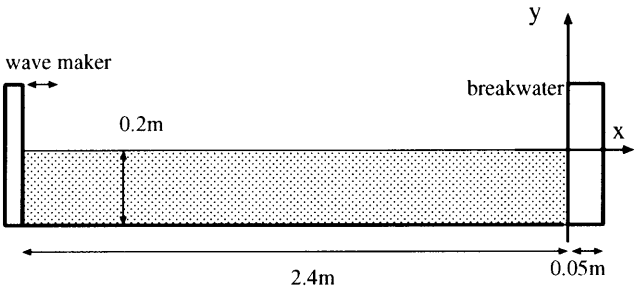

Fig. 18. Geometry for a breakwater

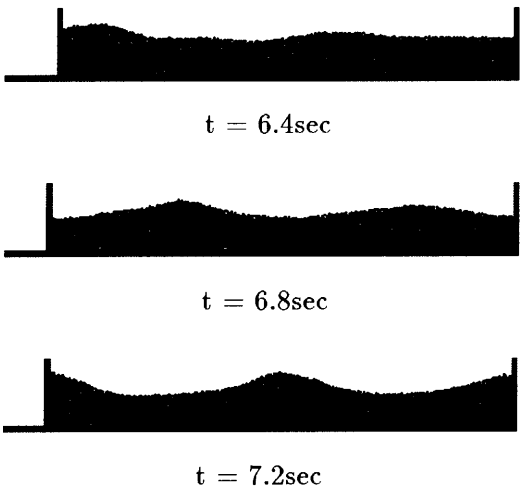

Fig. 19. Distribution of particles

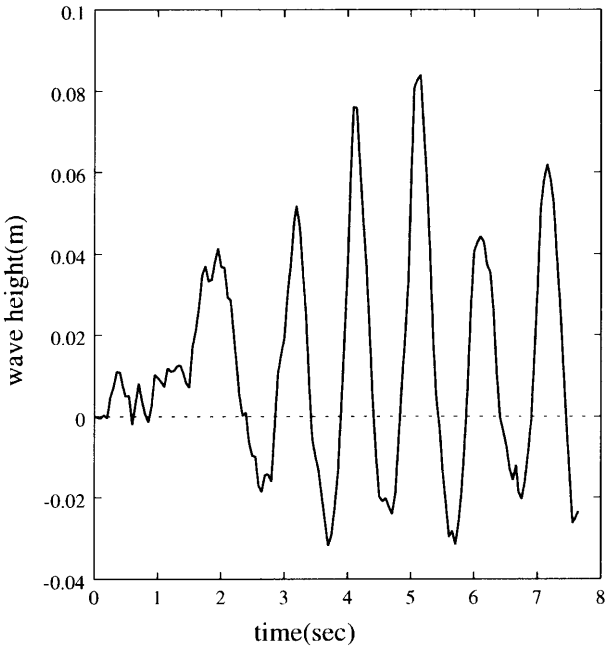

Fig. 20. Wave height at the breakwater

in Fig. 21. We can see a good agreement with the analytical solution which is estimated from the wave height using Sainfluo's theory. Figure 22 shows Sainflou's approximation (Sainflou 1928) of the pressure distribution on the

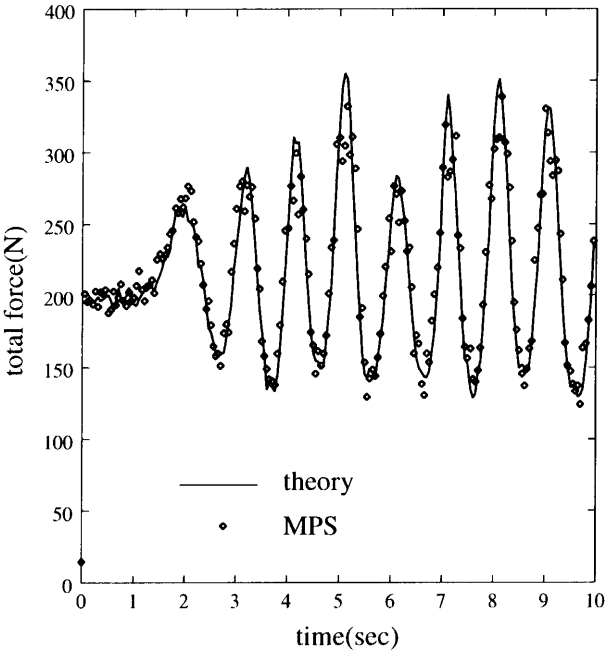

Fig. 21. Total force against the breakwater

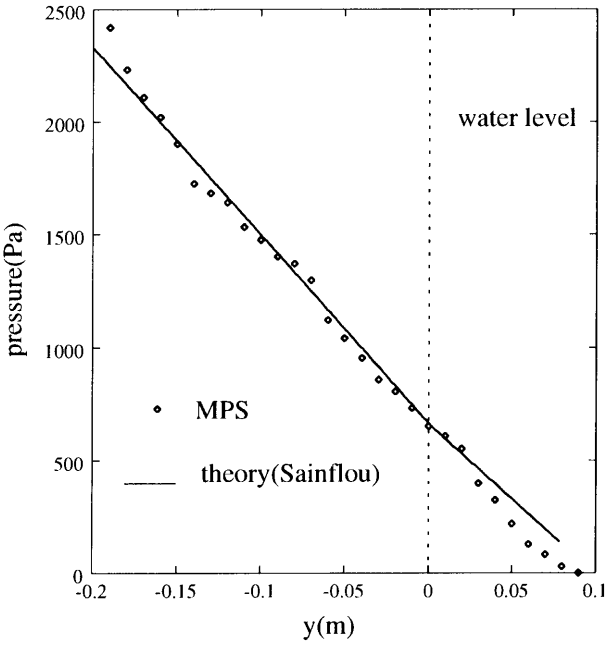

Fig. 23. Pressure distribution on the breakwater (5.16 s)

breakwater. When instantaneous average level at the breakwater is higher than the water level. The pressures p_1 and p_2 are

$$p_1 = (p_2 + \rho g h)\left(\frac{H + h_0}{H + h + h_0}\right)$$
$$p_2 = \rho g H\left\{1 + \frac{1}{\cos h(2\pi h/L)}\right\} \quad (37)$$

When the instantaneous is lower

$$p_1 = 0$$
$$p_2 = \rho g H\left\{1 + \frac{1}{\cos h(2\pi h/L)}\right\} \quad (38)$$

Figure 23 shows the pressure distribution on the breakwater when the wave height becomes the maximum at 5.16 s. It is also in good agreement with the theory. Displacement in the breakwater is shown in Fig. 24.

Fig. 24. Displacement of the breakwater ($\times 10^5$)

7 Conclusion

A new particle method for elastic and visco-plastic structures is developed. In this method, no element is used and particle interactions are modeled by the same way as MPS method which was developed for fluid flow analysis. Particles behave as if they are connected by normal and tangential springs. A tensile plate and a cantilever beam are solved by the present method. The results are in good

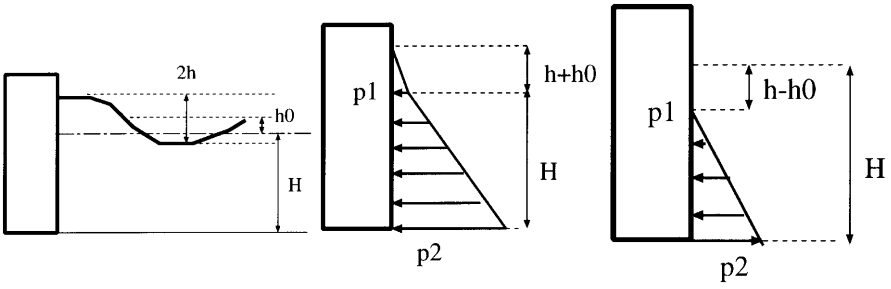

Fig. 22. Theoretical of pressure distribution (Sainflou 1928)

agreement with analytical solutions. The present method is also applied to visco-plastic structures. The calculated result of deformation of a visco-plastic bar agrees with analytical solution. Creep deformation and fracture of a cracked plate is calculated and the result is in good agreement with experiments.

This method is combined with MPS method for the analysis of fluid-structural interactions. Water falling on a cantilever beam is analyzed by the combined method. Impingement of water and resultant displacement of the beam are successfully obtained. Structural analysis in a breakwater and fluid flow analysis of waves are simultaneously carried out. The calculated pressure distribution on the breakwater is in good agreement with an analytical solution. The displacement distribution in the breakwater is also obtained.

The present study shows that the new particle method developed here can be applied to fluid structure interaction problems. Large deformation of interfaces will be solved without the mesh distortion using the present method. Such application, which should be accompanied by verification calculations, remains as a future study.

References

1. **Nayroles B, Touzot G, Villon P** (1992) Generalizing the finite element method: diffuse approximation and diffuse elements. Comput. Mech. 10: 307–318
2. **Belytschko T, Lu YY, Gu L** (1994) Element-free malerkin methods. Int. J. Num. Meth. Eng. 37: 229–256
3. **Yagawa G, Yamada T, Kawai H** (1996) Free mesh method: a new finite element method. Comput. Mech. 18: 383–386
4. **Atluri SN, Zhu T** (1998) A new meshless local Petrov-Galerkin (MLPG) approach in computational mechanics. Comput. Mech. 22: 117–127
5. **Atluri SN, Kim HG, Cho JY** (1999) A critical assessment of the truly meshless local Petrov-Galerkin (MLPG), and local boundary integral equation (LBIE) methods. Comput. Mech. 24: 348–372
6. **Atluri SN, Zhu T** (2000) New concepts in meshless methods. Int. J. Num. Meth. Eng. 47: 537–556
7. **Atluri SN, Sladek J, Sladek V** (2000) The local boundary integral equation (LBIE) and it's meshless implementation for linear elasticity. Comput. Mech. 25: 180–198
8. **Atluri SN, Zhu T** (2000) The meshless local Petrov-Galerkin (MLPG) approach for solving problems in elasto-statics. Comput. Mech. 25: 169–179
9. **Zhu T, Zhang JD, Atluri SN** (1998) A local boundary integral equation (LBIE) method in computational mechanics, and a meshless discretization approach. Comput. Mech. 21: 223–235
10. **Koshizuka S, Oka Y** (1996) Moving particle semi-implicit method for fragmentation of incompressible fluid. Nucl. Sci. Eng. 123: 421–434
11. **Koshizuka S, Nobe A, Oka Y** (1998) Numerical analysis of breaking waves using the moving particle semi-implicit method. Int. J. Num. Meth. Fluids 26: 751–769
12. **Koshizuka S, Ikeda H, Oka Y** (1999) Numerical analysis of fragmentation mechanisms in vapor explosions. Nucl. Eng. Des. 189: 423–433
13. **Gingold RA, Monaghan JJ** (1982) Kernel estimates as basis for general particle methods in hydrodynamics. J. Comput. Phys. 46: 429–453
14. **Chikazawa Y, Koshizuka S, Oka Y** (1999) Numerical analysis of sloshing with large deformation of elastic walls and free surfaces using MPS method. Transactions of the Japan Society of Mechanical Engineers, 65-637, A: 2954–2960
15. **Chikazawa Y, Koshizuka S, Oka Y** (1999) Development of an implicit particle calculation model for elastic structures. Proceeding of the Conference on Computational Engineering and Science (in Japanese) 4(1): 37–40
16. **Chikazawa Y, Koshizuka S, Oka Y** (1999) Numerical analysis of elastic structures using a particle method. The 12th Computational Mechanics Conference (in Japanese) pp. 723–724
17. **Koshizuka S, Chikazawa Y, Oka Y** (1999) Development of an explicit particle calculation model for elastic structures. Proceeding of the Conference on Computational Engineering and Science (in Japanese) 4(1): 33–36
18. **Koshizuka S, Chikazawa Y, Oka Y** (1999) Application of symplectic schemes to a particle model for elastic structures. The 12th Computational Mechanics Conference (in Japanese) pp. 725–726
19. **Nagashima T, Okuda Y, Yagawa M** (1996) Transactions of the Japan Society of Mechanical Engineers (in Japanese) 62–603, A: 2474–2480
20. **Yang TY** (1986) Finite element structural analysis, Prentice-Hall Inc.
21. **Sainflou G** (1928) Essai sur les diques maritimes verticales. Annales des Ponts et Chaussees, 98(1): 5–48
22. **Yokobori AT Jr, Yokobori T, Tabuchi M** (1996) The master curve and the constitutive equation for creep deformation and fracture for Cr-Mo-V steel throughout smooth, notched and precracked specimens. J. Mat. Sci. 31: 4767–4773